Advances in Natural Science **ISSN 1715-7862 [PRINT]**
Vol. **3**, No. **2**, **2010**, pp. 330-337 **ISSN 1715-7870 [ONLINE]**
www.cscanada.net **www.cscanada.org**

The 3rd International Conference of Bionic Engineering

Analysis of the Aerodynamic Character of Bionic Wingspan on the Basis of Frigate Wing Structure[1]

MA Yi[2]
LIU Yu-rong[3]
JIN Jing-fu[4]
CONG Qian[5]

Abstract: This paper extracts the frigate bird's leading edge contour by CATIA on the basis of the obverse and side pictures when frigate bird glides. Then three bionic wingspans of bending update, forward and integrating the two are built combining NACA 4412 airfoil. Compared with simple wingspan, the drag force of testing wingspan can be suppressed significantly, because the wingspan bending forward can form airflow of S style which declines the slope of the path-line of airflow and reduces the leading edge's pressures. As a result the working condition is improved because the bending forward wingspan reduces air's velocity. The lift efficiency of bending update wingspan may be improved because of increasing the leading edge's pressure resulting in high speed airflow.
Key words: leading edge contour; bionic wingspans; NACA 4412; aerodynamic performance

1. INTRODUCTIONS

Fig.1shows the frigate bird. It belongs to Pelecaniformes, frigate bird family. The wings range from 2 to 5 meters when spreads. The breast muscle is well developed. And the highest speed when predating is 400 kilometers per hour. It is the birds with the highest speed in the world[6]. The frigate wing has special characteristic of curved and long-narrow. This paper captures front and side pictures when

[1] **This work is supported by the National Natural Science Foundation of China (NO.50920105504), the Project of Technological Progress of Jilin Provenience (NO.20096032) and Basic Scientific Research Service Foundation of Jilin University.**
[2] Key Laboratory of Bionic Engineering, Jilin University, Ministry of Education, Changchun 130022, China
[3] Key Laboratory of Bionic Engineering, Jilin University, Ministry of Education, Changchun 130022, China
[4] Key Laboratory of Bionic Engineering, Jilin University, Ministry of Education, Changchun 130022, China
[5] Dr. Qian Cong, Key Laboratory of Bionic Engineering (Jilin University), Ministry of Education, Changchun 130022, People's Republic of China. E-mail: congqian@jlu.edu.cn.
[6] http://baike.baidu.com/view/36645.htm, 2010-6-2.
* Received 11 May 2010; accepted 29 July 2010

frigate bird glides through video. And the leading edge lines were extracted through pictures by CATIA. Then the space contour line combining the two lines was received by fitting of MATLAB. So are three bionic wingspans, which are bending update, forward and the two combining, using the lines above connecting airfoil of NACA4412. Compared with simple wingspan which is horizontal linear the aerodynamic characteristics of bionic wingspans were analysis through FLUENT. This paper aims at researching the aerodynamic characteristics of frigate wing profile, and extracting the general rules to provide some ideas for designing aircraft wings.

Fig. 1: Frigate bird[7]

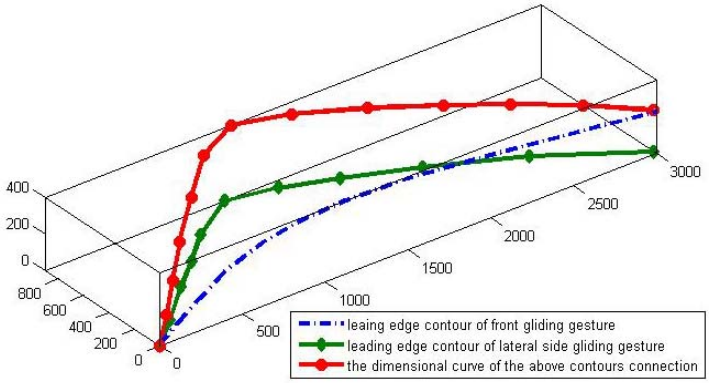

Fig. 2: Curves of the gliding gestures of frigate bird

2. EXTRACTING THE STRUCTURE OF FRIGATE WING AND REBUILD THE BIONIC WINGSPANS

Frigate belongs to the large-scale tropical seabird. Assumed that the width of wing is 3meters in CATIA, it extracts the tip contour features of front and side views when frigate is gliding. Integrating the front and side profiles together by MATLAB, the space profile line can be reached. Fig 2 is the graphical representation of front、lateral side edge profiles and the curve of the two connection. NACA 4412 wingspan is a normal one, which can be used to design the aircraft wing and leaves of wind turbines (GUILMINEAU, 1997). The ratio of wingspans length to airfoil hanging line is 3 to 1. Fig 3 is a simple wingspan using NACA4412. Fig 4 the bionic wingspans basing on the front profile line. Fig 5 is on the lateral side contour line. Fig 6 is on the combining line.

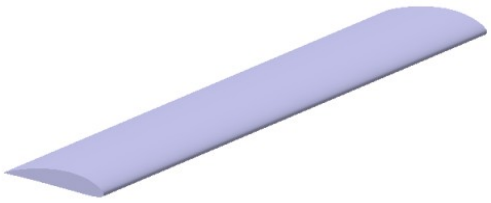

Fig. 3: Simple wingspan using NACA 4412 (model 1)

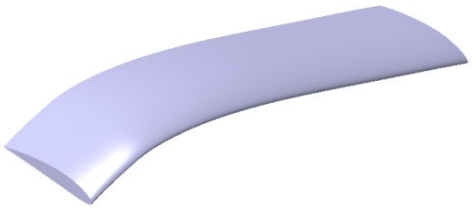

Fig. 4: Bionic wingspan basing on the front profile line (model 2)

[7] http://image.baidu.com/i?ct=503316480&z=&tn=baiduimagedetail&word=%BE%FC%BD%A2%C4%F1&in=26220&cl=2&lm=-1&pn=48&rn=1&di=1720019970&ln=1&fr=&ic=&s=&se=&sme=0, 2010-6-2.

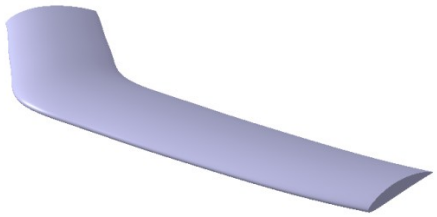

Fig. 5: Bionic wingspan basing on the on the lateral side contour line (model 3)

Fig. 6: Bionic wingspan basing on combining line (model 4)

3. NUMERICAL SIMULATIONS

Analysis is proceeded in the conditions of Re= 7.137×10^6 and the length of airfoil is 1 meter. Pressure far field is used as the boundary condition because air flow can be termed as compressed air flow when Ma=0.3[8]. Fig.7 shows the detailed scale of computation field and boundary conditions. C is the airfoil length in the figure. The Spalart-Allmaras model is the best model in single equation of fluent. The predicted values are close to the actual values when adverse pressure gradient is existing (Firooz, 2006). So the calculation result can be reasonable using this model. The boundary layers that cover airfoil are divided into viscous sublayer, buffer layer and log-low region (MA, 20009). The viscous drag is higher because of higher velocity gradient. Therefore, it's important to divide the grids into small ones nearby the wall and it's necessary that the y+<5 (Salim, 2009). The y+ number is less than 5 in this paper.

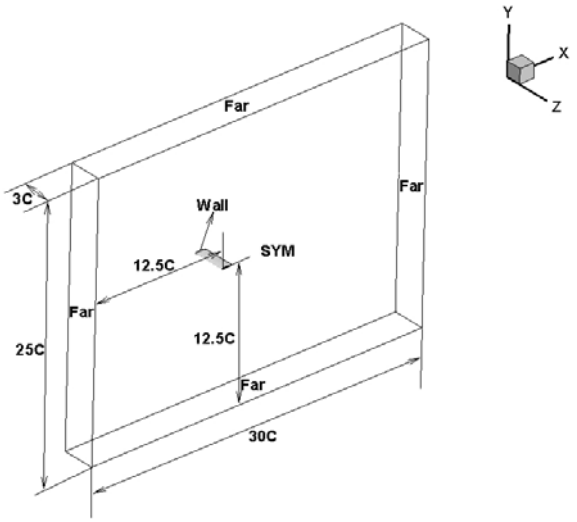

Fig. 7: The detailed scale of numerical field and boundary conditions

4. ANALYSIS OF THE SIMULATION RESULT

4.1 Simulation result

Fig.8 shows drag coefficients vary with angle of attack (AOA) of different wingspans. Drag coefficients reduce by 15% on average with a maximum of 18.9% for model 3 and model 4 compared with the simple one（model 1. The result indicates the structure of bending forward can reduce drag fore. Fig. 9 shows lift

[8] Fluent 6.2 Documentation File, ANSYS Manual, 2006.

coefficients change with AOA changes. The lift coefficient curve of model 2 is more stable than model 1 when AOA is greater than 10°. This indicates up-bend wingspan can improve lift efficiency. Fig.10 shows lift to drag coefficient varies with AOA. Lift coefficients of model 3 are smaller than others. The lift to drag coefficient is improved after connecting outlines of leading of model 2 and model 3. Effective union of the up-bend structure and forward can improve wingspans performance significantly from the above analyses.

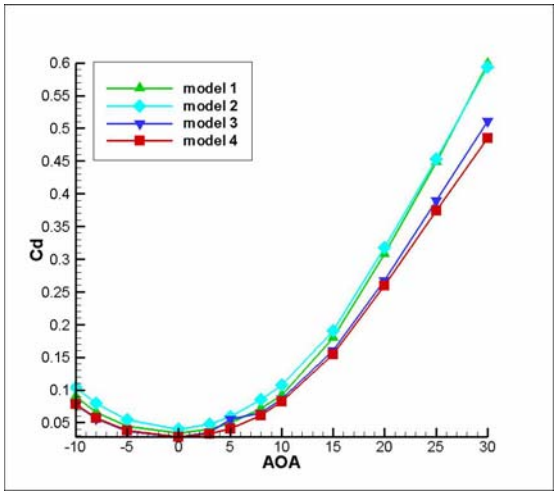

Fig. 8: Drag coefficients very with AOA changes

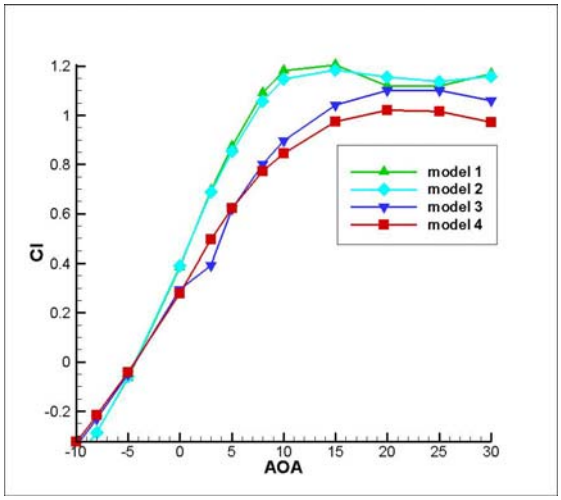

Fig. 9: Lift coefficients very with AOA changes

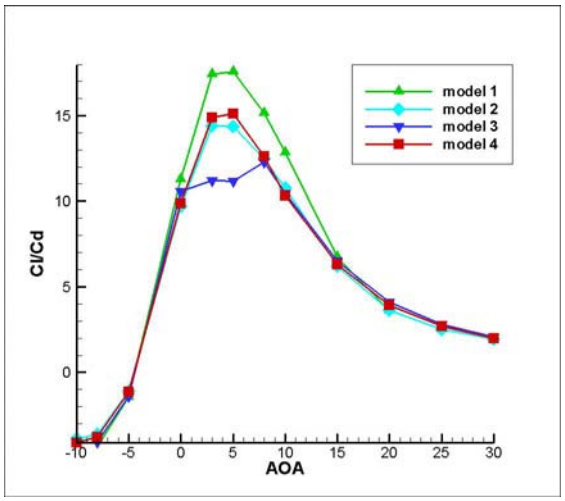

Fig. 10: Lift to drag coefficients very with AOA changes

4.2 Analysis of the simulation result

Fig.11 shows the path line of total pressure through all the wingspans when AOA equals 5°. The streamlines that flow over model 3 and model 4 become S style and are helpful to in reducing the intensity of pressure of the superficial of wingspans. The drag force along flow direction decreases because of the broke down of shear stress of wall. The lift efficiencies of model 3 and model 4 become are inferior than the model 1 and model 2. Because leading edge's maximum pressure of model 3 and model 4 decrease due to the reduction of airflow's velocity , which can decrease the pressure difference of the surface of upper and lower. The lift efficiency of model 2 is higher than model 1 due to the increase of leading edge's pressure which can improve airflow's velocity.

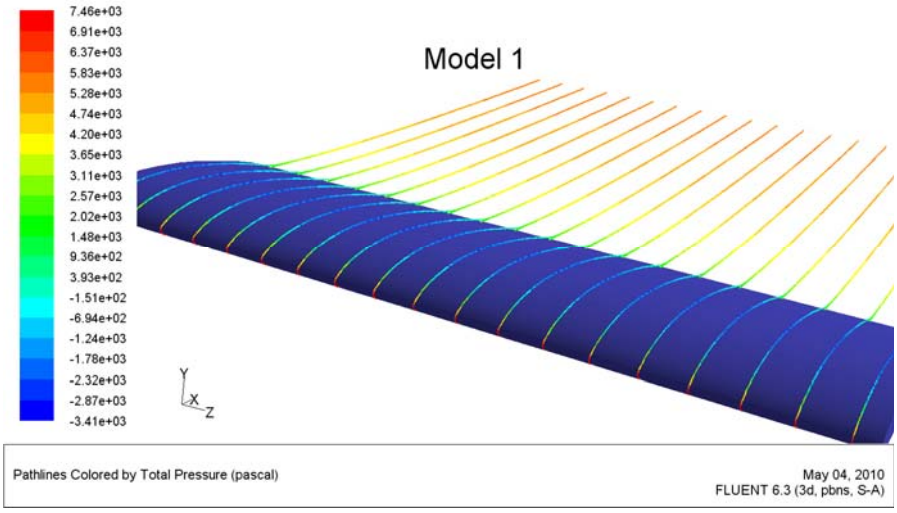
7.46e+03
6.91e+03
6.37e+03
5.83e+03
5.28e+03
4.74e+03
4.20e+03
3.65e+03
3.11e+03
2.57e+03
2.02e+03
1.48e+03
9.36e+02
3.93e+02
-1.51e+02
-6.94e+02
-1.24e+03
-1.78e+03
-2.32e+03
-2.87e+03
-3.41e+03
Model 1
Y
X
Z
Pathlines Colored by Total Pressure (pascal)
May 04, 2010
FLUENT 6.3 (3d, pbns, S-A)

(a)

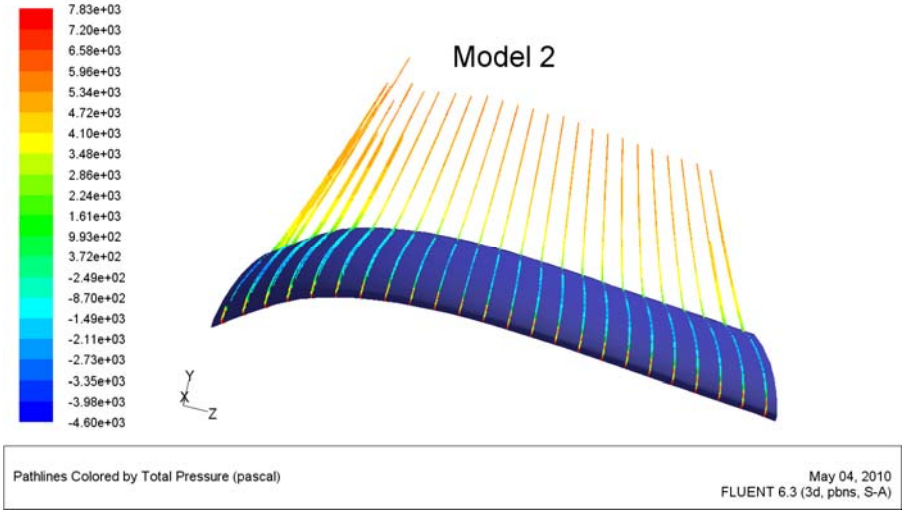
7.83e+03
7.20e+03
6.58e+03
5.96e+03
5.34e+03
4.72e+03
4.10e+03
3.48e+03
2.86e+03
2.24e+03
1.61e+03
9.93e+02
3.72e+02
-2.49e+02
-8.70e+02
-1.49e+03
-2.11e+03
-2.73e+03
-3.35e+03
-3.98e+03
-4.60e+03
Model 2
Y
X
Z
Pathlines Colored by Total Pressure (pascal)
May 04, 2010
FLUENT 6.3 (3d, pbns, S-A)

(b)

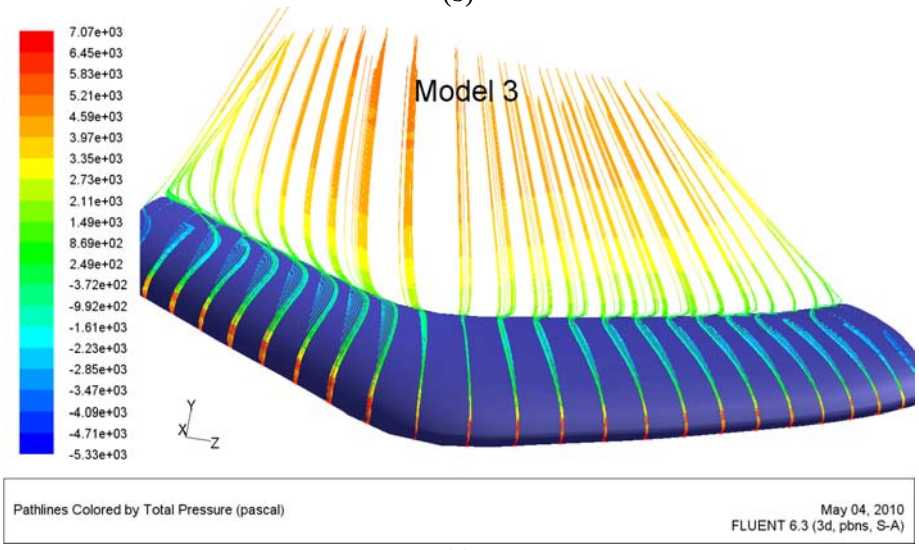
7.07e+03
6.45e+03
5.83e+03
5.21e+03
4.59e+03
3.97e+03
3.35e+03
2.73e+03
2.11e+03
1.49e+03
8.69e+02
2.49e+02
-3.72e+02
-9.92e+02
-1.61e+03
-2.23e+03
-2.85e+03
-3.47e+03
-4.09e+03
-4.71e+03
-5.33e+03
Model 3
Y
X
Z
Pathlines Colored by Total Pressure (pascal)
May 04, 2010
FLUENT 6.3 (3d, pbns, S-A)

(c)

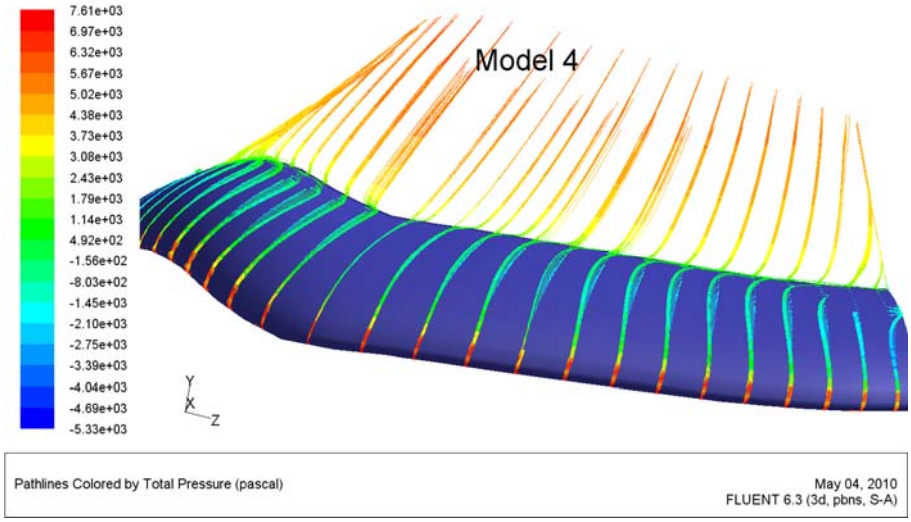

(d)

Fig. 11: Path-lines of total pressure when AOA=5°

Fig.12 presents velocity vectors flow over all wingspans when AOA equals 15°. Small eddy currents are formed upon the suction surfaces of model 1 and model 2. But it keeps laminar flow upon the surfaces of model 3 and model 4. The lift efficiency of model 1 and model 2 decreases quickly because of the increase of pressure that is leaded by small eddy currents (Tony & David, 2007). The drag force increases rapidly because that the turbulent flow expands the thickness of boundary layer (LU, 2009). By the sake of becoming turbulent flow in the late of the airflow in mode 3 and model 4 when AOA is larger than 15°, the lift efficiency of model 3 and model 4 changes positively than model 1 and model 2 gradually. From the analysis above, the forward- bending wingspan can improve the character of stall and working condition.

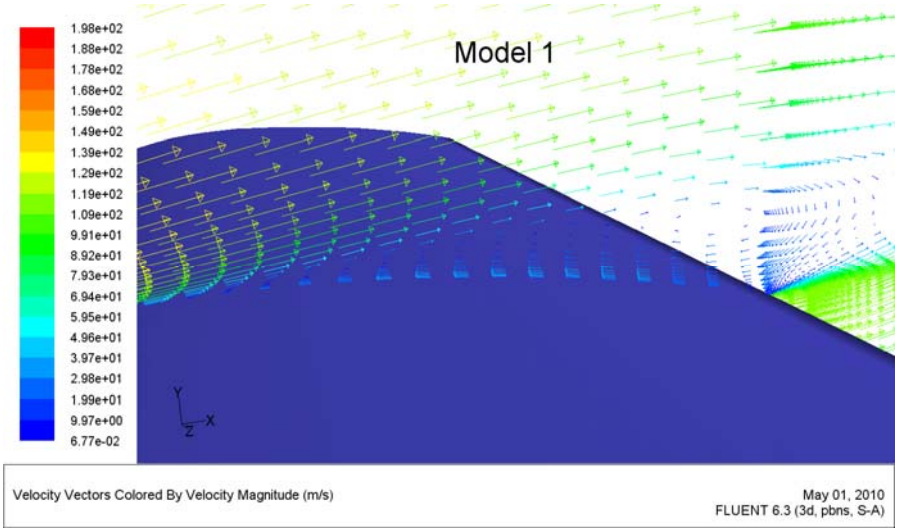

(a)

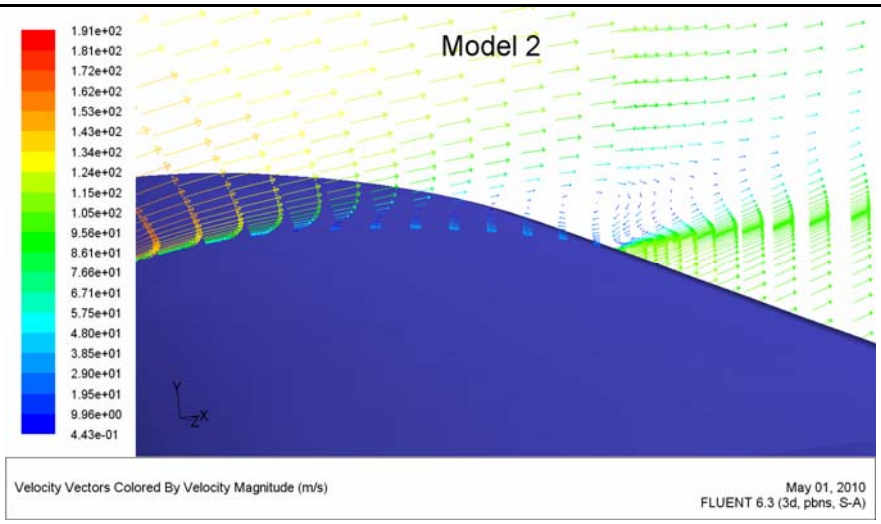

(b)

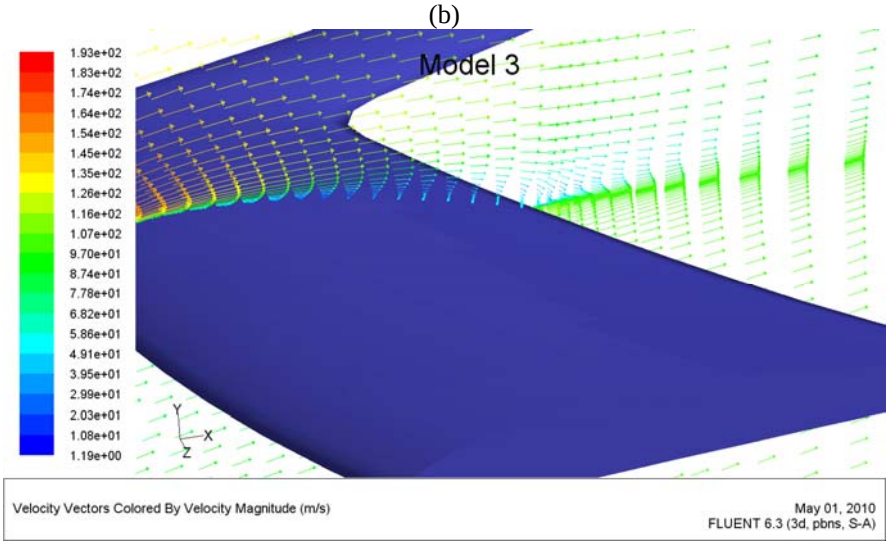

(c)

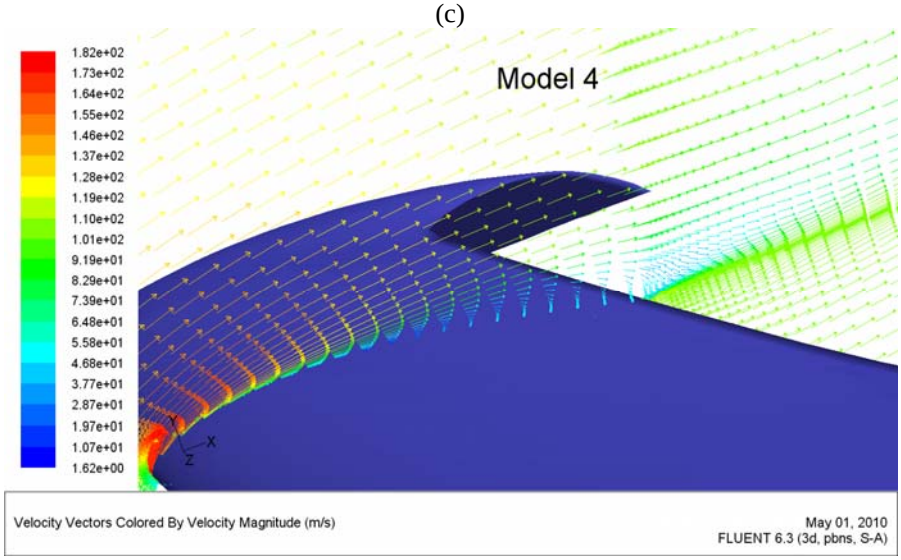

(d)

Fig. 12: Velocity vectors flow over wingspans when AOA=15°

5. CONCLUSIONS

(1) The drag force can be suppressed obviously because the wingspan of bending forward (model 3 and model 4) can form airflow of S style. This reduces the slope of airflow path line and the pressure of leading edge.

(2) The working condition may be improved because the wingspan of bending forward (model 3 and model 4) can improve the stall character because of reducing of airflow velocity.

(3) The lift efficiency of bending update wingspan can be improved due to that it can increase the leading edge's pressure resulting high speed airflow.

REFERENCES

A. Firooz. (2006). Turbulence Flow for NACA 4412 in Unbounded Flow and Ground Effect with Different Turbulence Models and Two Ground Conditions: Fixed and Moving Ground Conditions [C]. *Conference on Boundary and Interior Layers*: 98164-161.

E.GUILMINEAU. (1997). Two-Dimensional Turbulent Viscous Flow Simulation Past Airfoils at Fixes incidence [J]. *Elsevier Science, ,26(2)*: 135-162.

LU Zhiling. (2009). *Aerodynamics [M]*. Beijing: Beijing University of Aeronautics Press,8:117-127.

MA Rong. (2009). Numerical Simulation of Low-Reynolds-Number and High-Lift Airfoil S1223 [J]. *World Congress on Engineering, 2 (3)*: 1-6.

Salim. M. Salim. (2009). Wall y^+ Strategy for Dealing Wall-bounded Turbulent Flows[J]. *International MultiConference of Engineering and Computer Scientists, 3(2)*:18-20.

Tony Burton, David Sharpe.(2007). *Wind Energy Handbook* [M]. Beijing: Science Press:135-137.